

TEXTURE MODELING AND SIMULATION FOR SYNTHETIC PALM VEIN IMAGE GENERATION SYSTEM

Olajide Y. Adebayo^{1*}, Kudirat O. Jimoh¹, Esther O. Isola¹, Dimple T. Ogunbiyi¹, Segun Aina²

¹Osun State University, Osogbo, Osun-State, Nigeria

²Obafemi Awolowo University, Ile-Ife

olajide.adebayo@uniosun.edu.ng, kudirat.jimoh@uniosun.edu.ng, dimple.ogunbiyi@uniosun.edu.ng
s.aina@oauife.edu.ng

Abstract

Unavailability of large-scale palm vein databases due to their intrusiveness have posed challenges in exploring this technology for large-scale applications. Hence, this research modelled and generated synthetic palm vein images from only a couple of initial samples using statistical features. Variations were introduced to the three optimized statistical features (S5; the original images were employed as training images and the best variation in the first experiment as training images, S4; the best variation in the first experiment as training images while the original images were used as testing images, S3; mean vectors, covariance matrices and correlation coefficient, S2; mean vectors and covariance matrices, S1; mean vectors, Non-Synthetic; acquired image) which were used to generate synthetic palm vein images employing statistical and Genetic Algorithm (GA) approaches and were evaluated based on Equal Error Rate (EER), Average Recognition Accuracy (ARA) and Average Recognition Time (ART). The results obtained from the experiment showed that EERs were 0.22, 0.51, 0.58 and 4.36 for S3, S2, S1 and NS respectively. S3 had superior ARA (99.83%) compared with S2 (99.77%), S1 (99.70%) and NS (98.33%). The ARTs obtained were 84.97s, 75.55s, 84.04s and 681.74s for S1, S2, S3 and NS respectively with S2 (75.55s) having significantly least value. Furthermore, EER, ARA and ART for S4 were 0.43, 99.00%, and 12.13s, respectively while the corresponding values for S5 were 1.43, 97.50%, and 680.13s, respectively. The research outcome justifies the extraction of mean vectors, covariance matrices and correlation coefficient.

Keywords: Palm vein, Synthetic, Mean, Covariance, Correlation coefficient

1. Introduction

Large-scale biometric databases that include enough samples for training and testing are required for authentication systems. Most of the evaluations are based on a limited database since there are no public palm vein databases with sufficient samples. However, it is challenging to get palm vein images because they are highly intrusive (Lee, 2013), and it takes time and cooperation of subjects to gather sufficient palm vein data. A likely mitigation to these problems is working with synthetic biometrics. Several synthetic databases have been developed (Fingerprint (Cappelli *et al.*, 2002), Palmprint (Wei *et al.*, 2008), and Iris (Jinyu *et al.*, 2017) however, synthetic palm vein image generation has not at present fulfilled its undoubted potential. Hence, the aim of the study was to model and generate synthetic palm vein images from only a couple of initial samples by introducing variations to the statistical features (mean, covariance and correlation coefficient).

2. Related Works:

A method for synthetic fingerprint image generation using a mathematical model was developed by

Cappli *et al.* (2002). The randomly produced synthetic images have a limited number of parameters supplied to them. Acquisition devices produced an exceptional amount of variations, and Synthetic Fingerprint Generation (SFinGe) employed these to create a succession of prosthetic fingers, all with the same fingerprint. Synthetic fingerprints created from the method had a remarkable resemblance to genuine fingerprint, which was subsequently employed in fingerprint-based systems for performance evaluation. Realistic sensor-dependent backdrops were not included in the development of the ad-hoc stage.

Hadi *et al.* (2017) proposed an algorithm for creating a highly realistic synthetic datasets of pedestrians in a walkway as a substitute for real images. The synthetic images were fed to a designed Deep Convolutional Neural Network (DLCNN) to learn from. The result revealed that incorporation of synthetic data as a well-suited surrogate required exhaustive labeling.

Keke *et al.* (2018) leveraged on facial parts locations for better attribute prediction; a facial abstraction image which contained both local facial parts and facial texture information. Extensive evaluations

conducted showed that state-of the art performance was achieved. Future work would include integrating variations resulting from a change in viewing conditions. This would require rendering facial appearances using a face 3D model.

Bowen *et al.* (2019) developed a controllable text-to-image using a method called Control General Adversarial Network (controlGAN). This was achieved using word-level spatial and channel-wise attention-driven generator. They proposed a word-level discriminator to provide fine-grained supervisory feedback by collecting word with image region, facilitating training an effective generator which is able to manipulate specific visual attribute. Experimental results revealed the proposed method outperformed existing method in natural language description.

Michal *et al.* (2019) observed that images captured of football players during a football match had low resolution even when camera are of high resolution. They proposed an approach to resolve issue posed by low resolution image. Simple Python script for synthetic image was created instead of manual annotations. The raw synthetic images were transformed into more realistic image using Vanilla Cycle Generative Adversarial Network (CGAN) and trained using Cascade Pyramid Network (CPN) model. They were able to achieve similar precision with their images as the one of CPN model trained with Common Object in Context (COCO).

GAN was proposed by Islam and Zhang, 2020 for medical image synthesis. The method synthesizes brain images for Normal Control (NC), Mild Cognitive Impairment (MCI) and Alzheimer's disease (AD). The result showed that medical image synthesis using GAN is cost-saving approach for automated diagnostic technology.

Xuel *et al.* 2021 developed a model for synthesizing realistic histopathology image using HistoGAN. A synthetic framework that selectively adds new patches was also investigated. The developed models were evaluated on cervical histopathology and lymph node histopathology datasets. The results revealed that images generated with the developed model (HistoGAN) selective augmentation showed significant and consistent improvements.

Somasekar and Naveen, 2021 developed a synthetic image identification system GAN as a synthetic generator based on random sampling and Long Short term Memory (LSTM) as a discriminator. Facial datasets and abstract art datasets were used for training and testing. Accuracies were found to be 58.53% and 72.68% for both GAN and LSTM respectively.

Liu *et al.* (2021) evaluated the feasibility of deep learning method for fast reconstruction of synthetic Magnetic Resonance Imaging (MRI). Forty four subjects were used for training and fourteen for testing the model. Multiple Dynamic Multi-Echo Sequence (MDMES), Quantification maps and the magic software were employed for image acquisition, weighing and creation. Small error exists between generated and reference images. The study validated the deep learning method as a superior method for synthetic image generation.

3. Materials and Methods

This part presents the methodology employed in this research work. Palm vein images were acquired using M2SYS PalmSecure palm vein scanner. The second stage is the preprocessing procedure while low-cost method was used for features extraction. The features were selected and optimized by Genetic Algorithm (GA). Variation was introduced to the optimized features (S1; mean vectors, S2; mean vectors and covariance matrices, S3; mean vectors, covariance matrices and correlation coefficient, S4; the best variation in performance from the first experiment were employed as training images and the original images were used as testing images, S5, the original images were employed as training images and the best variation in performance from the first experiment were used as testing images) NS; acquired images to generate synthetic palm vein images as shown in Figure 1.

3.1 Image Acquisition

M2SYS PalmSecure palm vein scanner was used to capture 500 palm vein images of different subjects. All these images were stored in palm vein database and images served as training and testing datasets. The palm vein images acquired were fed as input to the preprocessing stage.

3.2 Preprocessing

The following sets of preprocessing steps necessary to improve the clarity of the vein pattern structure and localize the vein grid were applied;

3.2.1 Image Enhancement

A region of Interest (ROI) of 200 * 200 is extracted from the collected dataset. The palm images collected are often blur. The image firstly has to be enhanced to increase its contrast, and make the patterns more visible. Histogram equalization is used for image enhancement. In histogram equalization, the input pixel intensity, x is transformed to new intensity value, x^t by T . The transform function, T is the product of a cumulative histogram and a scale factor as presented in equation 1.

$$x^i = T(x) = \sum_t^x = 0^{n_i} \frac{\text{max intensity}}{N} \quad (1)$$

Where n_i is the number of pixels at intensity I , N is the total number of pixels in the image

3.2.2 Image Segmentation

The K-means algorithm is used for the segmentation stage after successful image enhancement with the histogram equalization. The algorithm is composed of the following steps:

v.

Let $X = \{x_1, x_2, x_3, \dots, x_n\}$ be the set of data points and

$V = \{v_1, v_2, \dots, v_c\}$ be the set of centers.

- i. Select 'c' cluster points randomly.
- ii. Compute the distance between each data point and cluster centers.
- iii. Assign the data point to the cluster center whose distance from the cluster centre is minimum of all the cluster centers.
- iv. Re-compute the new cluster center using:

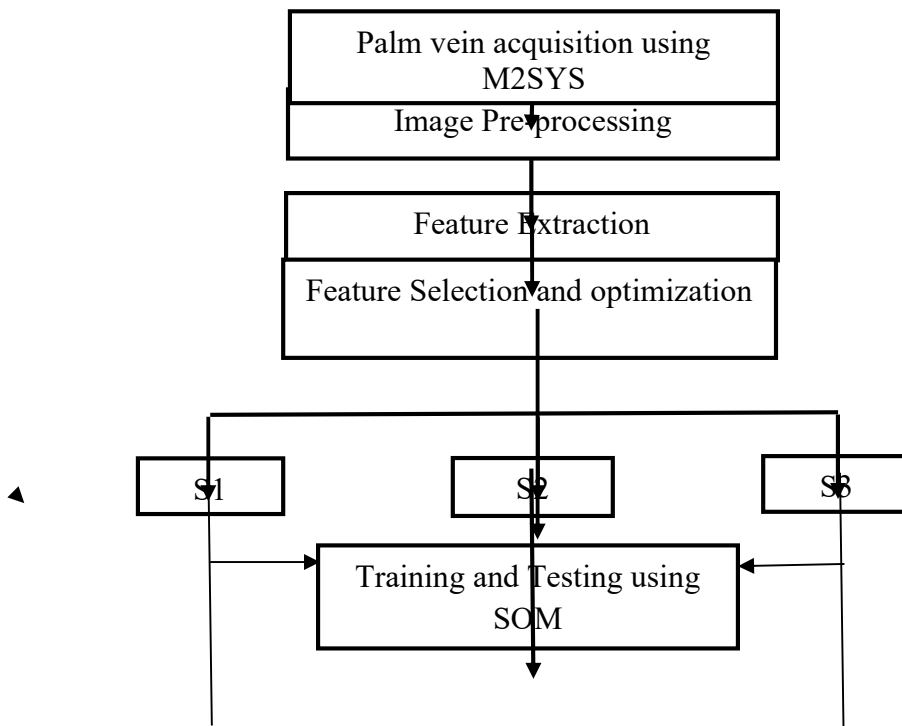


Figure 1 Block Diagram of the Developed Synthetic Palm Vein Image Generation System

$$j = \sum_j^k = 1 \sum_i^x = 1 \|x_t^{(f)} - c_j\|^2 \quad (2)$$

where, 'ci' represents the number of data points in i^{th} cluster.

- vi. Re compute the distance between each data point and new obtained cluster centers.

- vii. Stop if no data point was reassigned, else repeat from step c (Abikoye and Chukwu, 2016).

3.3 Feature Extraction

Mean, covariance and correlation coefficient of the normalized palm vein images were extracted using the low-cost method presented in Algorithm 1.

- i. Let X represent acquired palm vein with n rows and m columns. Let X^* represent

- synthetic palm vein to be generated, with n' rows and m columns.
- ii. X can be viewed as an $n \times m$ matrix and X' can be viewed as an $n' \times m$ matrix.
- iv.
- iii. The low-cost method presented in Algorithm 1 preserved the statistical properties of the normalized palm vein images X , in the reproduced synthetic palm vein images X' . (Eq. 3, 4 and 5).

Algorithm 1: (Low-Cost Method for Extraction of) of Statistical Properties

1. Generate A , which is a random $n' \times m$ matrix, such that the covariance matrix of A is the identity matrix.
2. Compute the covariance matrix C of the original data matrix X .
3. Use the Cholesky decomposition on C to obtain

$$C = U^t \times U \tag{3}$$

- where U is an upper triangular matrix and U^t is the transposed version of U .
4. Obtain the synthetic data set X' as a matrix product:

$$X' = A.U \tag{4}$$

Note That the covariance matrix of X' equals the covariance matrix of X .

5. Due to the construction of matrix A , the mean of each variable in X' is 0. In order to preserve the mean of variables in X , a last adjustment is performed. If \bar{x}_j be the mean of the j -th variable in X , then \bar{x}_j is added to the j -th column (variable) of X' :

$$x'_{ij} = x'_{ij} + \bar{x}_j \text{ for } i = 1, \dots, n' \text{ and } j = 1, \dots, m \tag{5}$$

Feature Selection (FS) ensures only relevant features of the palm vein images are used in the synthetic palm vein image generation process. As depicted in Algorithm 2, GA was employed for features selection. GA initially starts with a number of solutions known as population. These solutions were represented by using string coding of fixed length. After evaluating each chromosome using fitness function and assigning a fitness value, three different operators mutation, selection, and crossover were used to update the population. A repetition of these three operators is known as a generation. The new chromosome replaced the chromosome with the lowest survival rate.

Algorithm 2: Stepwise Procedure of the GA

1. Start
2. Get palm vein features set
3. Initialize parameters (set gen <= number of generations; set n <= population size, mutation probability)
4. Generate randomly distributed chromosomes to form initial population
5. Encode features by a chromosome {using bit strings encoding}
6. Gencount <= 0
7. Rank chromosomes based on its uniqueness {first chromosome occurrence = 1, subsequent occurrence = 0}
8. Arrange chromosomes based on their fitness value {Accept features with bit value = 1 and reject features with bit value = 0}
9. Mutate selected chromosomes based on mutation probability
10. Select chromosome with best fitness value
11. Perform crossover on parent chromosomes to form new offspring and replace the weak chromosomes with the new offspring
12. Gencount <= gencount + 1 and repeat until total number of generations
13. If gencount = gen then go to 14 else 7
14. Output chromosome with the highest fitness value (features selected)

3.4 Synthetic Palm Vein Image Generation

Figure 1 describes how synthetic palm vein images were generated. Mean, covariance and correlation

coefficient were three statistical features computed to derive synthetic palm vein images. Variations

were introduced to generate realistic synthetic palm vein as follows:

- a. S1 (Mean)
- b. S2 (Mean and Covariance)
- c. S3 (Mean, Covariance and Correlation Coefficient)

3.5 Experiments

In the first experiment, identification performances of each of S1, S2, S3 and NS (Original image) were conducted. For S1, statistical property (mean) was used for the synthetic palm vein image generation. For S2, statistical properties (mean and covariance) were used for the synthetic palm vein image generation. Finally S3, statistical properties (mean, covariance and correlation coefficient) were used for the synthetic palm vein image generation. In all SOM was used as classifier for all systems

considered. The flowchart showing the training and testing using SOM is presented in Figure 2.

The second experiment investigated measurement of similarities between the synthetically generated palm vein images and the original palm vein images. Synthetic palm vein images of the best variation in performance from the first experiment and all the original palm vein images were evaluated to determine their degree of similarities in their features. In S4, the synthetic images generated were employed as training images and the original images were used as testing images. However, in S5, the original images were employed as training images and synthetic images generated were used as testing images. The performance of the SOM on both trained and tested S1, S2 and S3 were evaluated based on EER, FAR, FRR, ART and ARA.

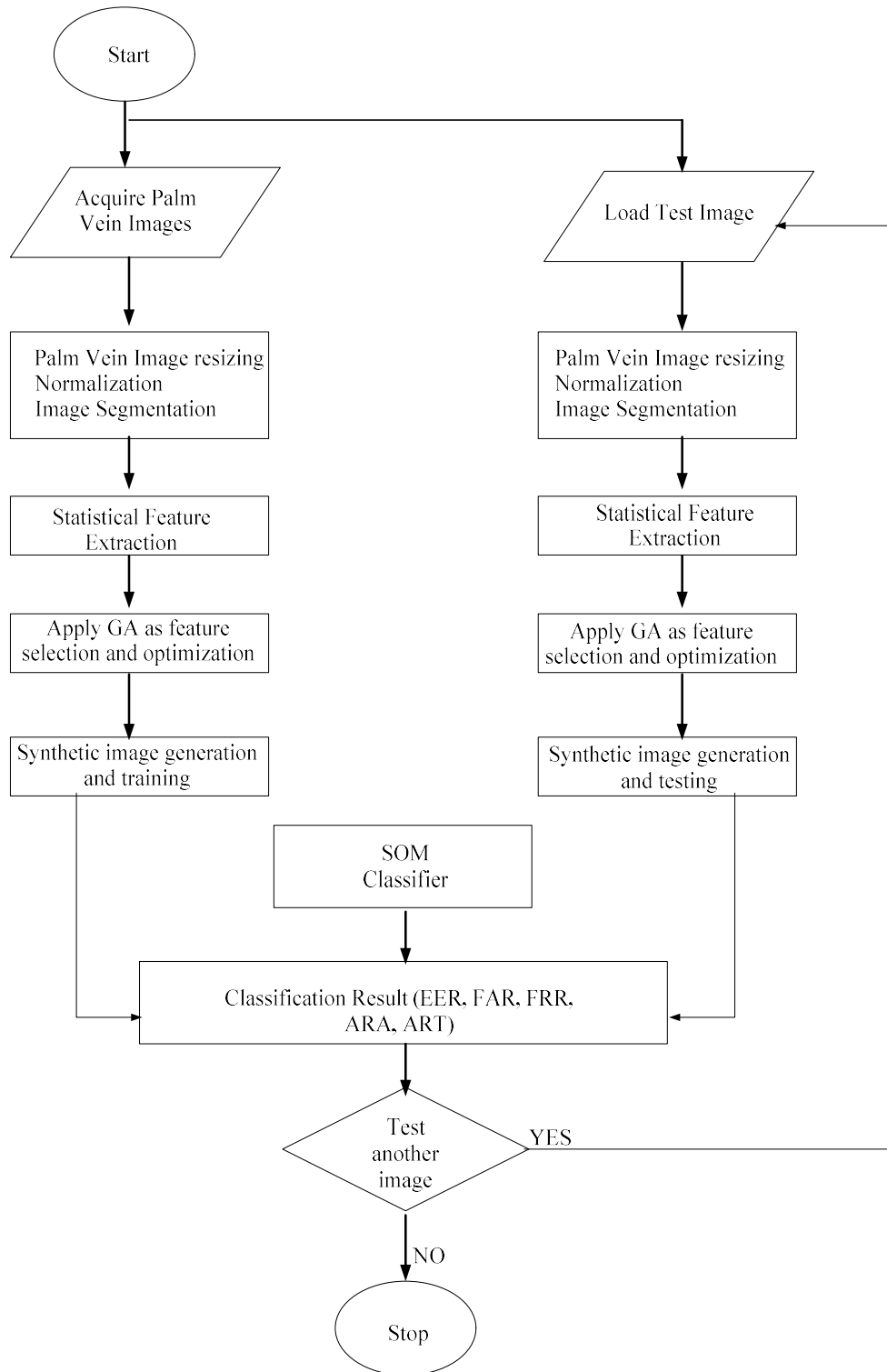


Figure 2: Flowchart showing Training and Testing using SOM

4. Results and Discussion

4.1 Results

The results of implementation of the synthetic palm vein generation system are presented in this section.

Table 1 Authentication Performance of the System

Synthetic Image Variation	ARA (%)	ART(s)	EER
NS	95.78	681.74	4.36
S1	99.68	84.97	0.58
S2	99.73	75.55	0.51
S3	99.80	84.04	0.22

Table 2: Estimated Similarity Measures for Synthetic and Acquired Images

Metric	S4 (Synthetic (Training) Original (Testing))	S5 (Synthetic (Testing) Original (Training))
EER	0.43	1.43
ARA (%)	99.00	97.50
ART (s)	12.13	680.13

Table 3: Test of significance on ART and ARA of the developed system

Parameter	Test	T	Degree of Freedom (<i>df</i>)	p-value	Comment
Accuracy	S3 vs S2	0.10667	8	0.000	Significant
	S3 vs S1	0.05222	8	0.000	Significant
	S3 vs NS	4.0122	8	0.000	Significant
ART	S3 vs S2	9.610	8	0.000	Significant
	S3 vs S1	-2.3822	8	0.001	Significant
	S3 vs NS	-598.806	8	0.000	Significant

Table 4: Test of significance for ARA and ART for S4 and S5

Parameter	Test	T	Degree of Freedom (<i>df</i>)	p-value	Comment
ARA	S4vs S5	5.994	8	.000	Significant
ART	S4vs S5	-4609.642	8	.000	Significant

4.2 Discussion

In Table 1, EER of the system under consideration were 0.22, 0.51, 0.58 and 4.36 for S3, S2, S1 and NS respectively. S3 has the least EER value in all the system under consideration, it exercised the topmost restraints to images that did not take part in the training and least restraints to training dataset. In view of this, it is the most secure and has the best performance because it is inbuilt with sufficient optimized statistical features.

In addition, ARA of 99.68% for S1; 99.73% for S2; 99.80% for S3; and 95.78% for Non-Synthetic. S3 had the highest ARA (99.80%) of system and this is on the basis that the more the optimized statistical features that were included training, the better average recognition accuracy. This is an indication that optimized statistical features (which are the mean, covariance and the correlation coefficient) with respect to the developed system contributed significantly to the overall performance as access control systems and/or identification systems.

ART obtained for the systems were 84.97s, 75.55, 84.04s and 681.74s for S1, S2, S3 and NS respectively, with S2 (75.55s) having significantly least value. This implied that the average rate of certifying the identity of an individual is significantly the least with respect to S2.

The second experiment was performed in order to measure the level of similarities of synthesized palm vein images with acquired original palm vein images, Table 2 showed the ARA of the two test sets of images with 99.00% for S4 (Synthetic images (training) and Original images (testing)) and 97.50% for the S5 (Original images (training) and Synthetic images (testing)). ART obtained for the images are 12.13s and 680.13s for S4 and S5 respectively. In addition, the EER was 0.43 for S4 and 1.43 for the S5. This implies that S4 has the best

access control performance, least time for certifying the identity of an individual and highest restraint to images that did not partake in training. Also, the original images employed in testing the system have enough statistical properties to match the training images which have only three statistical properties.

Consequently, in the first experiment, the validation of the performance of synthetic samples with respect to S1, S2, and S3 and the acquired sample images justifies the fact that the extraction of mean, covariance and correlation coefficient from the acquired palm vein images with *GA-SOM* as classifier significantly outperformed acquired palm vein. Moreover, in the second experiment, S4 (Synthetic (training samples) Original (testing samples)) was found to be significantly better in performance than S5 (Original (training samples and Synthetic (testing samples))). The main reason for S4 significant performance (with respect to all the metrics used) over S5 could be attributed to the fact that each of the original images used as a test sample inherently has all the statistical properties to match the synthetic palm vein images (which only contains three statistical properties) used in training. This confirmed that statistically synthetic images once generated, can be populated efficiently enough to serve as the training sample while the original palm vein images can be employed as the test sample.

The *p-value* for ARA and ART were 0.000 and 0.000 respectively. The *p-value* depicts statistical significance at $P < 0.01$. Test of significance of the ARA and ART evaluated at 95% confidence level shows that there was significant difference between the synthetic and acquired sample palm. Hence the alternative hypothesis is accepted. The t-test result validates the fact that synthetic outperformed the acquired palm sample in terms of ARA and ART.



Figure 3: Samples of Acquired Palm Vein Images

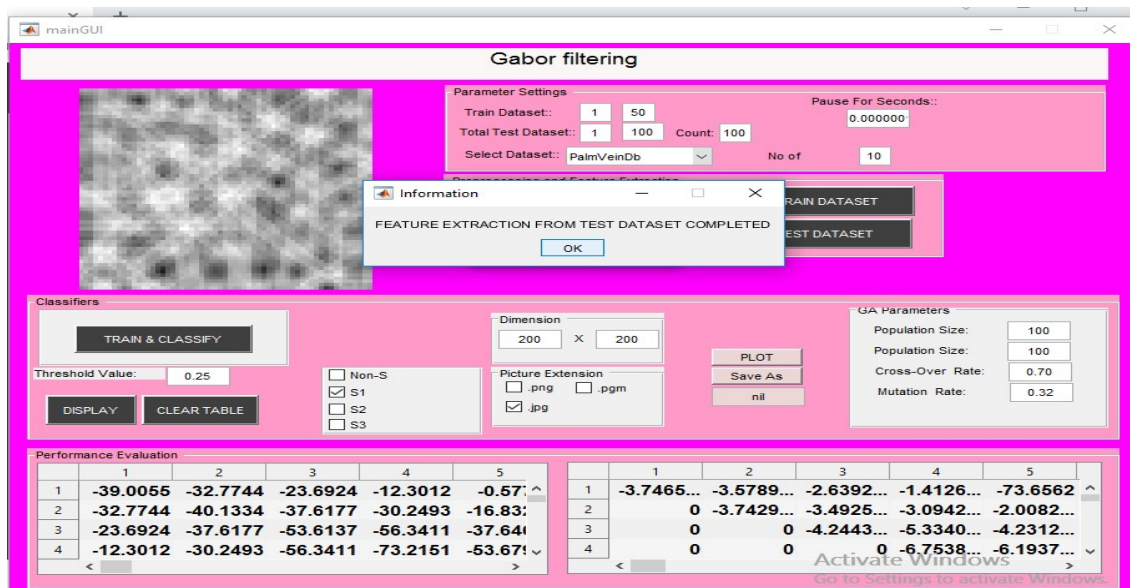


Figure 4: Samples of Feature Extracted from Palm Vein Images

5. Conclusion

Realistically, an indication of optimized statistical features contributed significantly to the overall performance of synthetic palm vein image generation. Also, this confirmed that statistically synthetic images once generated, can be populated efficiently enough to serve as train sample while the original palm vein images can be employed as test sample. Conclusively, the work has presented a method to create a synthetic palm vein database, which is reasonable facsimiles of real palm vein images

References

Abikoye, O. C, and Chukwu, M. (2016). An Improved Palm Vein Based Recognition System Computing. Information Systems,

Journal of Development Informatics and Allied Research, 7(1): 21-28.

Bowen, L. Xiaojuan, Q. Thomas, L. Philip H. S. (2019). Controllable Text-to-Image Generation. 33rd Conference on Neural Information Processing Systems, Vancouver, pp. 1-11.

Cappelli, R. Maio, D. and Maltoni, D. (2002). Synthetic Fingerprint-Database Generation. 16th International Conference on Pattern Recognition. Québec City, pp. 744-747.

Hadi, K. Ekbatani, O. Pujol and Santi Segui (2017). Synthetic Data Generation for Deep Learning in Counting Pedestrians. 6th

- International Conference on Pattern Recognition Applications and Methods, pp. 318-323.
- Jinyu Zuo, Natalia A. Schmid and Xiaohan Chen (2017) "On Generation and Analysis of Synthetic Iris Images, Information Forensics and Security, IEEE Transactions 2(1): 77-90.
- Somasekar, H and Naveen, K. (2021). A System for Identifying Synthetic Images Using LSTM: A Deep Learning Approach. International Journal of Computer Trends and Technology, 69(2):64-67.
- Islam, J. and Zhang, Y. (2020). GAN-Based Synthetic Brain PET Image Generation. Brain Informatics, 7(3):1-12.
- Keke, H. Yanwei, F. Wuhao, Z. Chengjie, W. Yugang, J. Feiyue, H. Xiangyang, X. (2018). Harnessing Synthesized Abstraction Images to Improve Facial Attribute Recognition. Proceedings of the Twenty-Seventh International Joint Conference on Artificial Intelligence, pp. 733- 740.
- Lee, Y. P. (2013). Palm Vein Recognition Based on a Modified (2D) 2LDA. Journal of Signal, Image and Video Processing, 9(1):229-242.
- Mengyi, L. Zhiyong, Y. Yufeng, M. Xingwei, C. and Qian, Y. (2012). Heterogeneous Face Recognition and Synthesis Using Canonical Correlation Analysis. Journal of Information Technology, 7(8):398- 407.
- Milan, B. and Martin, D. (2016). Generation of Skin Diseases into Synthetic Fingerprints. International Journal of Image Processing, 10(5):229-248.
- Michal, S. Grzegorz, S. and Tomasz, T. (2019). Synthetic Image Translation for Football Players Pose Estimation. Journal of Universal Computer Science, 25(6):683-700.
- Liu, Y. Haijun, N. Pengling, R. Jialiang, R. Xuan, W. Wenjuan, L. Heyu, D. Jing, L. Jingjing, X. Tingting, Z. Han, L. Hongxia, Y. and Zhenchang, W. (2022). Generation of Quantification Maps and Weighted Images from Synthetic Magnetic Resonance Imaging using Deep Learning Network, Institute of Physics and Engineering in Medicine, 67:1-12.
- Wei Zhuoshi, Yufei Han, Zhenan Sun and Tieniu Tan (2008): "Palmpoint Image Synthesis", A Preliminary Study, ICIP 15th IEEE International Conference on Image Processing, 285-288.
- Yuan Xue, Jiarong Ye, Qianying Zhou, L. Rodney Long, Sameer Antani, Zhiyun Xue, Carl Cornwell, Richard Zaino, Keith C. Cheng, Xiaolei Huang (2021). Selective Synthetic Augmentation with HistoGAN for Improved Histopathology Image Classification, Medical Image Analysis 67:101816.